Journal of Mining and Environment (JME) Vol. 12, No. 4, 2021, 1189-1203

Shahrood University of Technology

Iranian Society of Mining Engineering (IRSME)

Journal of Mining and Environment (JME)

journal homepage: www.jme.shahroodut.ac.ir

THOMSON REUTERS

A Modified Indirect Boundary Element Analysis for Fatigue Behavior Assessment of Rock-Like Materials Based on Linear Elastic Fracture Mechanics

Rezvan Alizadeh[1], Mohammad Fatehi Marji[1*], Abolfazl Abdollahipour[2], Mehdi Pourghasemi Sagand[1]

1- Department of Mining and Metallurgical Engineering, Faculty of Engineering, Yazd University, Yazd, Iran.
2- School of Mining Engineering, College of Engineering, University of Tehran, Tehran, Iran

Article Info

Received 1 December 2021
Received in Revised form 7 December 2021
Accepted 16 December 2021
Published online 16 December 2021

DOI:10.22044/jme.2022.11534.2139

Keywords

Fatigue crack propagation
Mixed-Mode condition
Stress intensity factor range
Cyclic loading

Abstract

In this work, an effective methodology is introduced for modeling the fatigue crack propagation in linear elastic brittle media. The displacement discontinuity method is used to accomplish the analysis, and the boundaries are discretized with quadratic elements in order to predict the stress intensity factors near the crack tips. This procedure is implemented through 2D linear elastic fracture mechanics. The normal and shear displacement discontinuity around the crack tip is applied to compute the mixed-mode stress intensity factors. The crack growth is incremental, and for each increment of extension, there is no need to use a re-meshing procedure. This method has benefits over the finite element method due to its simplicity in meshing. The crack growth direction is assessed using the maximum principal stress theory. In these analyses, a repetition method is used in order to estimate the correct path of crack propagation. Therefore, the different lengths of incremental growth do not affect the crack growth path analysis. The results are exhibited for several examples with different geometries to demonstrate the efficiency of the approach for analyzing the fatigue crack growth. The accuracy represents that this formulation is ideal for describing the fatigue crack growth problems under the mixed-mode conditions.

1. Introduction

In the analysis of rock engineering and the construction process, which involves the rock material, there is not only static loading but also the rocks are frequently subjected to repeated and dynamic loading, especially in the highway and railway projects [1–3]. These resulting cyclic stresses can lead to a microscopic damage to the material involved [4]. Even at the stresses well below a rock's ultimate strength, this microscopic damage can accumulate, and lead to failure [5]. This process of damage due to cyclic loading is called the fatigue of rock. Due to the long-term impact of cyclic loading, the strength of rock is steadily reduced. Therefore, the safety of structures is affected [6].

There are three special techniques for examining and designing averse to fatigue failures. The traditional stress-based technique is according to stress. Another technique is the strain-based technique, which utilizes localized yielding criteria that may happen during cyclic loading. Besides, there is the fracture mechanics technique, which investigates crack propagation by the fracture mechanics principles [7]. The natural rock mass includes numerous flaws and defects such as cracks and joints. Due to the brittleness and elastic behavior of most rock materials, the fracture mechanics technique can be effectively used to study the fatigue mechanism in these materials [8, 9]. Indeed, the presence of a crack can significantly reduce the strength of the material due to brittle

Corresponding author: mohammad.fatehi@gmail.com (M. Fatehi Marji).

fracture, and crack growth can be caused by cyclic loading, which is called the fatigue crack growth behavior [10, 11].

The numerical method has a high precision in modeling the fatigue procedures based on the fracture mechanics principle. The restrictions of the analytical and empirical methods in realistic and intricate issues, particularly in fracture mechanics, have caused the fast development of the numerical methods in this field [12, 13]. The domain-based methods have critical restrictions in explaining the solid mechanics problems associated with a continuous alteration in geometry [14]. The crack propagation phenomenon is an example in which the application of these methods needs a re-meshing procedure to illustrate the ideal growth path [15, 16]. This procedure makes numerical methods difficult and often causes decreases in the precision and convolution of computer programing. In the meantime, the boundary element method has been demonstrated to be a powerful numerical approach, which has essential superiorities to domain-based techniques. The significant characteristic of this method is that it requires just a discretization of the boundaries. Different formulations of the boundary integral methods have been extended for the elastic fracture mechanic problems. These techniques utilize various approaches when encountering singularities of stress close to crack tips [17]. Cen and Maier (1992) have simulated crack propagation in concrete with BEM [18]. Ingraffea *et al*. (1987) and Grestle (1986) have introduced the mixed-mode crack propagation situations with the BEM for two- and three-dimensional problems [19, 20]. They applied the multi-region technique with the maximum circumferential stress criterion to estimate the crack growth path. Doblare *et al*. (1990) have utilized the multi-region technique with the quarter-point element to simulate crack propagation in the orthotropic substances [21]. In the incremental propagation of the crack, the artificial boundaries of the multi-region technique must be frequently presented for each increment of growth [22]. These boundaries, which are used to separate the domains, are not unique, and they cannot be easily performed in automatic processes [23]. Accordingly, the Dual Boundary Element Method (DBEM) with a single region technique has been introduced for the two- and three-dimensional crack problems, respectively, by Portela *et al*. (1993) [24] and Mi and Aliabadi, 1994, 1995 [25, 26]. The crack growth procedure can be modeled using the new element in this method. Aliabadi (2002) has presented a general review of the DBEM applications [17]. The fatigue crack propagation of anti-symmetric cracks has been analyzed using DBEM and FEM [27]. Leonel and Venturini have utilized DBEM for the multiple crack propagation analyses [28]. Besides, the indirect boundary element method is another technique that utilizes the superposition principles. This kind of BEM includes the Fictitious Load Method (FLM) and the Displacement Discontinuity Method (DDM) [29]. DDM has been introduced by Crouch and Starfield (1983) [30]. The constant form of this method is simple, and widely used in the engineering analysis [31–34]. DDM has been developed for the static and dynamic 2D/3D problems [35–37]. This technique has been widely utilized for a range of engineering problems such as explosive fracturing, rock cutting, hydraulic fracturing, and rock stability [38–42].

In this work, a methodology for analyzes of fatigue crack growth in linear elastic regions is presented. As explained in the following section, this technique utilizes the displacement discontinuity of quadratic elements in order to compute the range of stress intensity factor distributions for each crack in the domain. This parameter is then applied to predict the crack propagation rates. The constant cyclic loading is applied considering the mixed-mode condition. Besides, an incremental crack growth scheme is proposed to model the crack length increment at each progressive step of the domain with different crack growth rates.

The more fundamental fracture criteria have been introduced to implement the fatigue propagation path based on the fracture mechanic principle. Some of these criteria are based on the stress approach, and others are established on the energy approach. The minimum strain energy density criterion (S criterion) [43], maximum circumferential stress criterion (σ criterion) [44], and maximum strain energy release rate criterion (G criterion) [45] are the most popular theories to use in brittle materials. The σ theory demonstrates that the crack growth is accomplished when the maximum tangential stress achieves its critical value in the substance. Due to the simplicity of this procedure, the stress theory has been evaluated as the easiest criteria to understand and apply [46]. This criterion has been widely applied in the fracture mechanic problems [46, 47]. Therefore, in this research work, the propagation path of a fatigue crack is determined through the maximum circumferential stress criterion. Besides, a repetition algorithm is also used to predict the

correct direction. This algorithm makes it possible to obtain a single crack path using the growth increments with different lengths.

2. Description of numerical method

The displacement discontinuity method is developed through analytical solutions like another BEM. This numerical method constructs a discrete approximation of a continuous distribution of displacement discontinuity (DD) along a segment [48]. A general DD distribution is exhibited along the x-axis in Figure 1a. This technique considers DD as normal, and parallels to the segment surface (indeed, deformation resulting from the opening and shearing modes of fracturing). Crouch and Starfield (1983) have defined the primary format of this technique [30]. In their template, the displacement discontinuity tolerates a constant specified change when crossing from one side to the other side. Accordingly, DD ($D_{x\,\&\,y}$) can be written as follows (Figure 1b):

$$\begin{cases} D_x = u_x(x,0^-) - u_x(x,0^+) \\ D_y = u_y(x,0^-) - u_y(x,0^+) \end{cases} \quad (1)$$

The analytical integration of quadratic shape functions over linear displacement discontinuity elements is the quadratic element basis [49]. Therefore, the displacement discontinuity function can be written in a general form as:

$$D_i(\varepsilon) = N_1(\varepsilon)D_i^1 + N_2(\varepsilon)D_i^2 + N_3(\varepsilon)D_i^3 \quad i = (x,y) \quad (2)$$

where D_i^1, D_i^2, and D_i^3 are the quadratic nodal displacement discontinuities, and:

$$\begin{cases} N_1(\varepsilon) = \dfrac{\varepsilon(\varepsilon - 2a_3)}{8a_3^2} \\ N_2(\varepsilon) = -\dfrac{(\varepsilon^2 - 2a_3^2)}{4a_3^2} \\ N_3(\varepsilon) = \dfrac{\varepsilon(\varepsilon - 2a_3)}{8a_3^2} \end{cases} \quad (3)$$

are the shape function for the equal sub-elements ($a_1 = a_2 = a_3$). The displacements and stresses for a crack in a body along the axis, considering the single harmonic functions ($f(x,y)$ and $g(x,y)$), are given based on Eq. (4) and Eq. (5) [49]:

$$\begin{aligned} u_x &= [2(1-\vartheta)f_{,y} - yf_{,xx}] + [-(1-2\vartheta)g_{,x} - yg_{,xy}] \\ u_y &= [2(1-\vartheta)f_{,x} - yf_{,xy}] + [2(1-\vartheta)g_{,y} - yg_{,yy}] \end{aligned} \quad (4)$$

and:

$$\begin{aligned} \sigma_{xx} &= 2G[2f_{,xy} + yf_{,xyy}] + 2G[g_{,yy} + yg_{,yyy}] \\ \sigma_{yy} &= 2G[-yf_{,xyy}] + 2G[g_{,yy} - yg_{,yyy}] \\ \sigma_{xy} &= 2G[2f_{,yy} + yf_{,yyy}] + 2G[-yg_{,xyy}] \end{aligned} \quad (5)$$

where G is the shear modulus, ν is the Poisson's ratio, and $g_{,xyy}$, $f_{,xyy}$, $f_{,y}$, $g_{,yy}$ … are the partial derivatives of the harmonic functions (f *and* g). The potential functions for a quadratic element are obtained by [50].

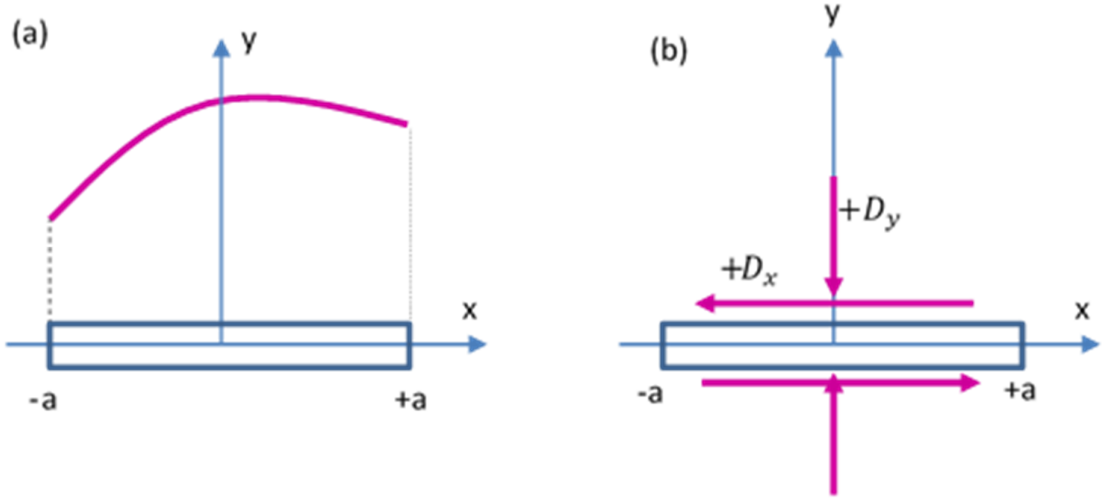

Figure 1. a) General displacement discontinuity distribution of constant element b) Components of constant displacement discontinuity ($D_{x\,\&\,y}$).

$$f(x,y) = \frac{-1}{4\pi(1-\vartheta)} \sum_{j=1}^{3} D_x^j F_j(I_i)$$
$$g(x,y) = \frac{-1}{4\pi(1-\vartheta)} \sum_{j=1}^{3} D_y^j F_j(I_i) \quad (6)$$
$$i = (0\ to\ 3)$$

in which the function F_j is specified as:

$$F_j(I_0, I_1, I_2) = \int N_j(\varepsilon) \ln[(x-\varepsilon)+y^2]^{0.5}\, d\varepsilon \quad (7)$$
$$j = 1\ to\ 3$$

The integrals $I_i (i = 0\ to\ 2)$ are defined according to Eqs. (8) to (10).

$$I_0(x,y) = \int_{-a}^{+a} ln[(x-\varepsilon)^2 + y^2]^{0.5} d\varepsilon = y(q_1 - q_2) - (x-a)\, ln(r_1) + (x+a)\, ln(r_2) - 2a \quad (8)$$

$$I_1(x,y) = \int_{-a}^{+a} \varepsilon ln[(x-\varepsilon)^2 + y^2]^{0.5} d\varepsilon = xy(q_1 - q_2) + \frac{1}{2}(y^2 - x^2 + a^2)\, ln\frac{r_1}{r_2} - ax \quad (9)$$

$$I_2(x,y) = \int_{-a}^{+a} \varepsilon^2 ln[(x-\varepsilon)^2 + y^2]^{0.5} d\varepsilon = \frac{y}{3}(3x^2 - y^2)(q_1 - q_2) + \frac{1}{3}(3xy^2 - x^3 + a^3)\, ln(r_1) + \frac{1}{3}(3xy^2 - x^3 - a^3)\, ln(r_2) - \frac{2a}{3}\left(x^2 - y^2 + \frac{a^2}{3}\right) \quad (10)$$

The phrases q_1, q_2, r_1, and r_2 are defined as follow:

$$q_1 = tan^{-1}\left(\frac{y}{x-a}\right)$$
$$q_2 = tan^{-1}\left(\frac{y}{x+a}\right) \quad (11)$$

$$r_1 = [(x-a)^2 + y^2]^{0.5}$$
$$r_1 = [(x+a)^2 + y^2]^{0.5} \quad (12)$$

The partial derivatives of these integrals have been presented in the literature [51]. The high-stress concentration adjacent to the tip in the brittle material causes severe changes in the stress and displacement. Therefore, distributions of these parameters in these regions are different from the other area. Owing to the singularity variations of the stresses and displacements in the proximity of the crack tip, the precision of the method reduces. Accordingly, it is necessary to utilize the crack tip element in the analyses. A particular crack tip element that has been already introduced in [30] is applied in the proposed algorithm. Thus the variations of displacement discontinuity along with a crack tip element with a length of 2a are exhibited as [50] (Figure 2).

$$D_x(\varepsilon) = D_x(a)\left(\frac{\varepsilon}{a}\right)^{0.5}$$
$$D_y(\varepsilon) = D_y(a)\left(\frac{\varepsilon}{a}\right)^{0.5} \quad (13)$$

Dx(a) and Dy(a) are the opening and shearing displacement discontinuities at the center of the crack tip element, and ε is the distance from the tip. The potential functions $f_c(x,y)$ and $g_c(x,y)$ for the crack tip element are specified as:

$$f_c(x,y) = \frac{-1}{4\pi(1-\vartheta)} \int_{-a}^{+a} \frac{D_x(a)}{a^{0.5}} \varepsilon^{0.5}\, ln((x-\varepsilon)^2 + y^2)^{0.5}\, d\varepsilon$$
$$g_c(x,y) = \frac{-1}{4\pi(1-\vartheta)} \int_{-a}^{+a} \frac{D_y(a)}{a^{0.5}} \varepsilon^{0.5} \ln((x-\varepsilon)^2 + y^2)^{0.5}\, d\varepsilon \quad (14)$$

By considering the typical elements i and j along the boundary of the problem, moreover, by substituting Equations 6, 14, and other related equations of them in displacement and stress equations, the general solution is determined (Eq. (15)). Finally, the normal and shear boundary conditions are defined according to the displacement discontinuity, and influence the coefficients ($C_{SS}(i,j), C_{nn}(i,j), \ldots$).

$$\begin{cases} b_s^i = \sum_{j=1}^{N} C_{SS}(i,j) D_s^j + \sum_{j=1}^{N} C_{Sn}(i,j) D_n^j \\ b_n^i = \sum_{j=1}^{N} C_{nS}(i,j) D_s^j + \sum_{j=1}^{N} C_{nn}(i,j) D_n^j \end{cases} \quad (15)$$
$$i = 1\ to\ N$$

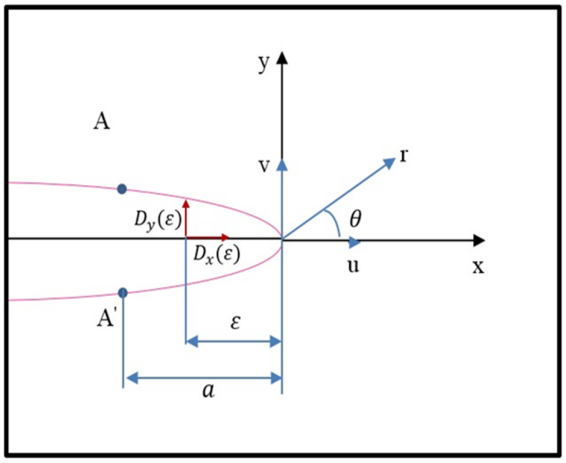

Figure 2. Displacement discontinuity distribution of a particular crack tip element.

3. Fatigue crack growth considering linear elastic fracture mechanics

The solution process for the fatigue crack growth problem starts with the evaluation of the entire boundary element discretization using DDM. For each load of constant amplitude cyclic loading (maximum and minimum), a mechanical response is determined through the system. Consequently, the stress intensity factors for mode-I and mode-II are easily computed based on the normal and shear displacement discontinuity of each crack tip element [49] (Eqs. (16) and (17)).

$$K_I = \frac{G}{4(1-\vartheta)}\left(\frac{2\pi}{a}\right)^{0.5} D_y(a) \tag{16}$$

$$K_{II} = \frac{G}{4(1-\vartheta)}\left(\frac{2\pi}{a}\right)^{0.5} D_x(a) \tag{17}$$

In the DDM analysis, the crack growth is simulated by successive linear increments. Therefore, the propagation path and the size of increments must be specified. Various techniques have been established in the research works for determining the crack growth in the mixed-mode conditions. Due to the simplicity and capability of preparing a precise estimation, the maximum circumferential stress theory is employed in the present investigation (σ-criterion). Erdogan and Sih have expressed that in the case of plane strain or generalized plane stress where the brittle material contains a crack, the stresses in the proximity of the crack tip are written considering LEFM, as follow [44]:

$$\begin{cases} \sigma_\theta = \frac{1}{\sqrt{2\pi r}} cos\frac{\theta}{2}\left[K_I cos^2\frac{\theta}{2} - \frac{3}{2}K_{II}\, sin\,\theta\right] \\ \tau_{r\theta} = \frac{1}{2\sqrt{2\pi r}} cos\frac{\theta}{2}\left[K_I sin\theta + K_{II}(3cos\theta - 1)\right] \end{cases} \tag{18}$$

Based on this criterion, the crack extension is perpendicular to the direction of maximum principal stress of the crack tip. Therefore, considering Eq. (18), if $\tau_{r\theta} = 0$:

$$K_I sin\theta_m + K_{II}(3cos\theta_m - 1) = 0 \tag{19}$$

θ_m is the direction of crack propagation. This angle is calculated using the stress intensity factor, as follows:

$$\theta_m = sin^{-1}\left[\frac{K_I K_{II} - 3K_{II}\sqrt{8K_{II}^2 + K_1^2}}{9K_{II}^2 + K_I^2}\right] \tag{20}$$

This theory is a continuous criterion. In a discretized numerical process, it does not consider the alteration of the stress field in the crack propagation; Consequently, there is no certainty that the estimated crack path is unique. Therefore, a repetitive-improver plan is used, which considers the stress conditions at the developed crack tip. This scheme re-estimates the crack growth angle until the true path is attained [24]. In this plan, the modification angle (φ) is applied in order to determine the actual propagation direction of the crack. The procedure is shown for the nth step of crack extension in Figure 3. The modification angle (φ) is expressed based on the geometry:

$$\varphi = \frac{\theta_{m(n+1)}}{2} \tag{21}$$

in which, $\theta_{m(n+1)}$ is the crack propagation angle for the next increment that is calculated with the σ criterion. This scheme is repeated until the new modification angle is smaller than the previous modification angle. Indeed, in determining the progress direction of the nth step of extension, an iterative process is applied as follows:

1. The angle of crack growth (θ_m) is estimated in the first iteration using the σ criterion (Eq. 20.)
2. The crack is extended in size da to the new tip (c^i) along the direction calculated in the previous step, and then the new stress intensity factors are calculated.
3. A new crack direction ($\theta^i_{m(n+1)}$) is predicted through the criterion and the new stress intensity factors.
4. Then the modification angle is computed through Eq. 21.
5. The angle of the nth step is modified as:

$$\theta_{m(n+1)}^{i+1} = \theta_{m(n+1)}^{i} + \varphi^{i} \quad (22)$$

6. This procedure is iterated from phase 2 with the direction of the modified angle until the modification angle is greater than the previous modification angle. In this condition, the direction is the final propagation angle ($|\varphi^{i+1}| \geq |\varphi^{i}| \Rightarrow \theta_{m(n+1)}^{i+1} = \theta_f$).

The correction angle is negligible when the length of increment tends to zero. Consequently, the propagation path has a propensity to the direction of the tangent of the continuous track. The growth rate of a crack under cyclic loading is usually specified as a function of the stress intensity factor range (ΔK). Many formulate for this relationship exist but the Paris-Erdogan laws [52] is used here as the earliest and simple formulation, which is written as:

$$\frac{da}{dN} = C(\Delta K)^m \quad (23)$$

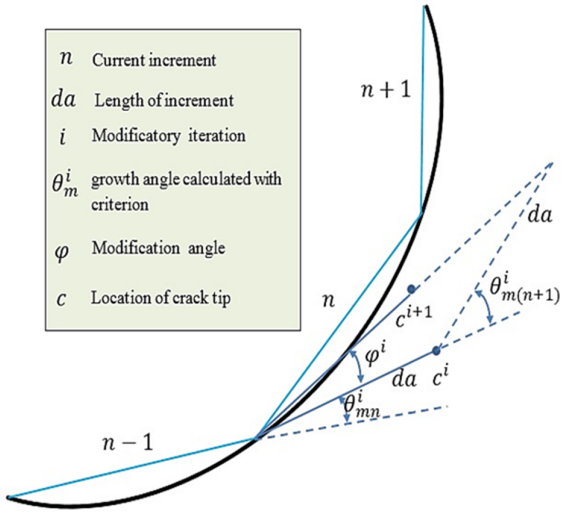

Fig 3. Applying the correction angle to improve the nth crack propagation increment of extension.

where c and m are the materials constant, a is the crack length, and N is the number of load cycles. The range of the stress intensity factor for the mixed-mode condition is determined through the experimental equation (Eq. 24):

$$\Delta K = (\Delta K_I^4 + 4\Delta K_{II}^2)^{0.25} \quad (24)$$

ΔK_I and ΔK_{II} is determined through the difference between the stress intensity factor of each mode, which is computed for a maximum and minimum load of a constant amplitude loading. For multiple cracks in a structure, the increment for each crack is defined based on the maximum growth rate, which leads to the following:

$$\Delta a = \Delta a_{max} \frac{c\Delta K^m}{\left(\frac{da}{dN}\right)_{critical}} \quad (25)$$

$\left(\frac{da}{dN}\right)_{critical}$ is the greatest crack propagation rate among all the different crack tips in the simulation. Δa_{max} is the maximum crack length increment, and it is equal to the reference increment, which is determined for each analysis. In a problem with various cracks, the life is assessed considering the tip with the highest propagation rate. Therefore, the fatigue life (in terms of the cycle) for each extension step is expressed by:

$$\Delta N = \int_0^{\Delta a_{max}} \frac{da}{C(\Delta K_{max})^m} \quad (26)$$

The fatigue growth processes of the proposed method take place when the crack propagation rate prevails the threshold stress intensity factor range (ΔK_{th}); otherwise, propagation does not occur. Besides, in the condition that the maximum value of ΔK of each extension step is greater than K_{Ic} of material, the impermanent growth happens, which is called a material fracture, and the failure and process is stopped. The following phases present the fatigue crack growth procedure of the proposed methodology:

1. During the displacement discontinuity analysis, the values of the stress intensity factor of each crack tip are determined through the normal and shear displacement discontinuities.
2. The range of stress intensity factor is calculated for all crack tips.
3. The crack growth rate of each crack tip is determined through the range of stress intensity factor.
4. The life of the structure (based on the load cycles) required for crack length extension is assessed. In a problem involving different cracks, the number of load cycles is specified considering the crack with the highest growth rate.

The increments of extension for each crack tip are determined considering their growth rate.

5. The crack propagation direction is determined based on the σ-criterion and according to the values of the stress intensity factor of each crack tip.
6. The position of the crack tips is updated according to their increment and the propagation angle.

7. A new DDM analysis is accomplished, and the new stress intensity factors and crack propagation path for the next progression step are calculated.
8. Using the growth direction of the next step, the propagation angle of the nth step is modified.
9. The growth directions of the cracks are updated, and this process is repeated from phase 5 to get the most suitable propagation path for all the tips.

4. Numerical applications for validation of proposed method

In this section, the numerical examples have been exhibited that are used as validation and represent the application of the method explained in the previous section. The first example is about the propagation of a single crack under cyclic loading. This example investigates the crack growth in the mixed mode conditions, and also considers the influence of the modified σ -criterion in the propagation path. The second example examines two parallel-interior cracks located at a different level. As described in the following, each application is developed as a fatigue crack propagation problem that predicts the crack growth path and domains life based on cycles using the proposed method.

4.1. Propagatioon of single crack under cyclic load

This application includes the fatigue growth of a rectangular plate consisting of an inclined crack, which is exhibited in Figure 4a. The cyclic load is supposed as $\sigma_{max} = 172.37\, MPa$ and ratio $R = 0.1$ (Figure 4b). The maximum load was considered in a way that the radius of the plastic area around the crack tip was nearly less than 10% of the specimen dimensions. Thus the hypothesis of small-scale yielding was utilized. Figure 4 represents the dimensions and boundary conditions of the rectangular specimen. The dimensions utilized in the numerical modeling are hight = 304.8 mm, width = 76.2 mm, and crack length (2a) = 14.2 mm. The angle of the inclined crack respecting to the horizon is $\gamma = 60^o$, and the material parameters are assumed as E = 128 GPa and $\nu = 0.31$. Besides, the material constant for the fatigue law is $C = 1.5 \times 10^{-9}$, $m = 3.8$.

In order to accomplish the numerical analysis, the boundaries was discretized into 46 elements, while the plane of the crack was divided into 8 elements; two of them were the crack tip elements. Besides, a size of increment for crack tip is equal to 0.5 mm, which is utilized to perform the crack propagation analysis under cyclic loading.

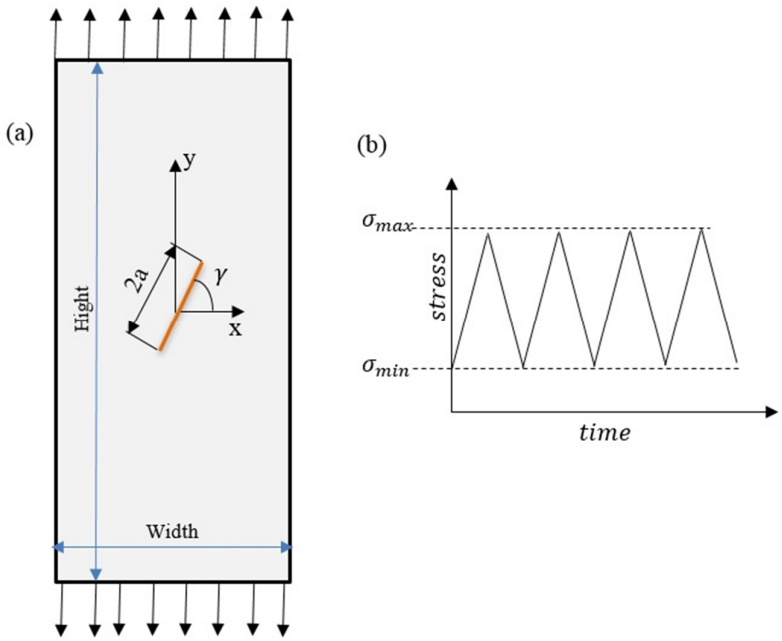

Figure 4. Details of single crack under cyclic loading (a) Geometry and boundary conditions, (b) Distribution of applied cyclic loadin.

Figure 5. represents the crack propagation path for both crack tips through the proposed technique during 15 growth increments. These analyses were performed for the increments with the length of 0.5 mm, in which the crack growth direction was based on the standard and modified criteria. The data of

the experimental test of this specimen is also presented in this figure [53]. Due to the symmetry conditions of the problem, the results of the numerical simulations for both crack tips (left and right) are similar, while the empirical data shows a partial difference. As it is clear, the results of the two criteria (standard and corrected) do not match, and after ten increments of growth, these differences are entirely clear. Among these results, the growth path curve of the modified criterion is much more compatible with the data of experimental examination.

Figure 6. exhibits the analysis based on the increments of 1.25 mm in length. In this scenario, the cracks passed the growth path using six increments. The progressive step has been increased for 2.5 times. Nevertheless, the results of the modified criterion still have a high accuracy and do not differ much from the experimental results.

For a better comparison, the data for both analyzes of the right crack tip are displayed at a higher magnification in Figure 7. The figure demonstrates that usage of the modified criterion in the fatigue crack growth with different sizes of increment ultimately leading to a single crack path. In the simulations in which the correction coefficient was not applied, the higher the length of increment, consequently, the higher error in the crack growth path.

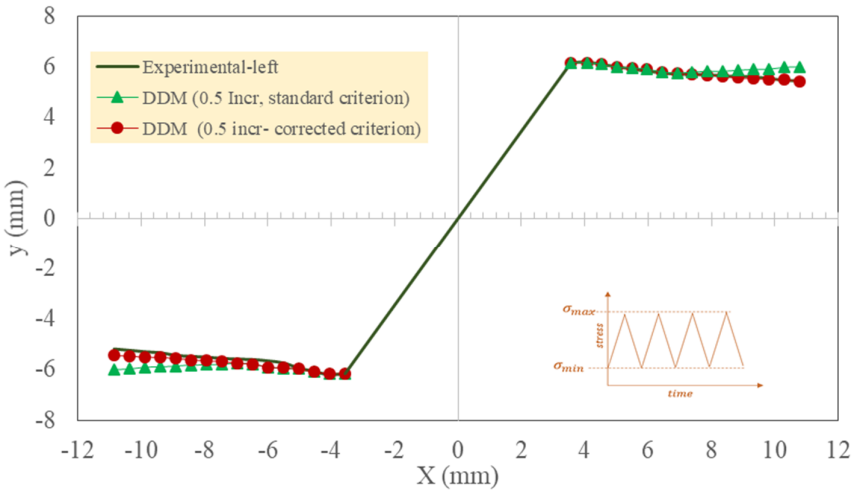

Figure 5. crack trajectory with incremental growth of 0.5 mm implemented by σ-criterion, modified σ-criterion, and experimental tests

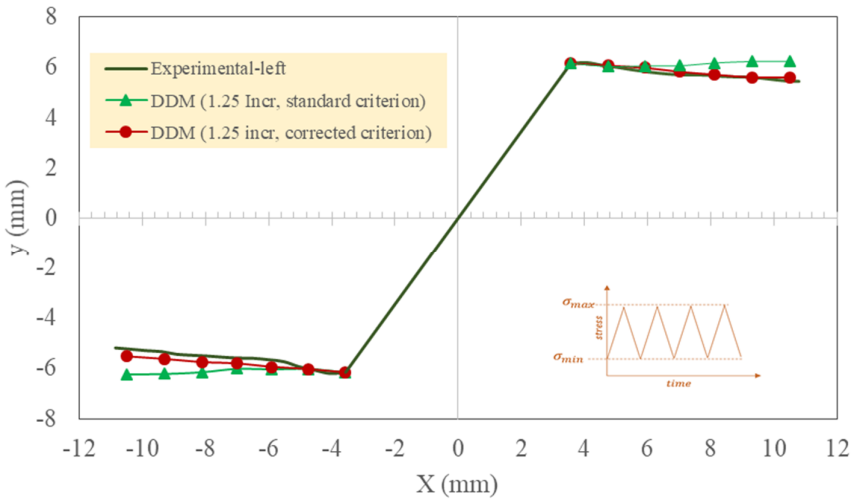

Figure 6. Crack trajectory with incremental growth of 1.25 mm implemented by σ-criterion, modified σ-criterion, and experimental tests.

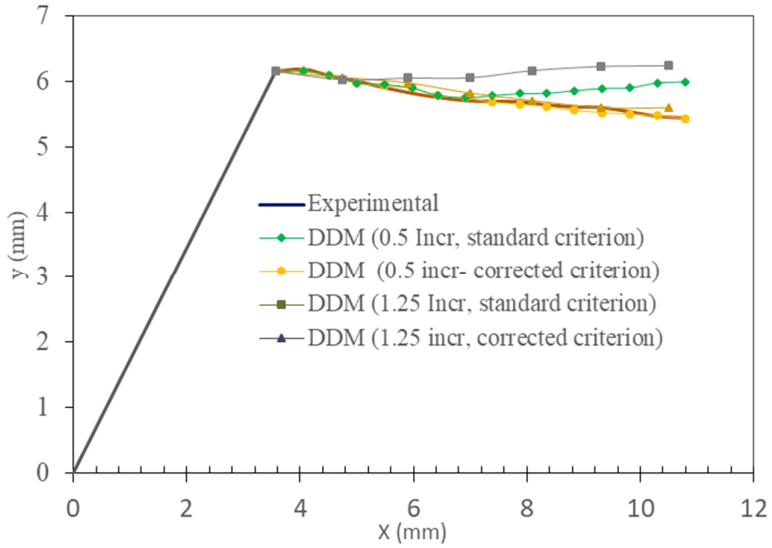

Figure 7. Comparison of growth trajectory of single crack under cyclic loading with different lengths of increment and different criteria for crack propagation.

Figure 8 displays the life determined by the proposed DDM. This curve is based on an incremental length of 0.5 mm. Each crack tip through the 7300 load cycles extended to the length of 14.612 mm. Due to the symmetry of the example, the growth rates are also the same for both crack tips in the numerical results. This figure also exhibits the results determined by the empirical tests. The results of the two tips are slightly different, in a way that the left crack tip extended to 13.972 mm and the right tip extended to 13.932 mm. The results acquired from the DDM analysis have a good agreement with the experimental data.

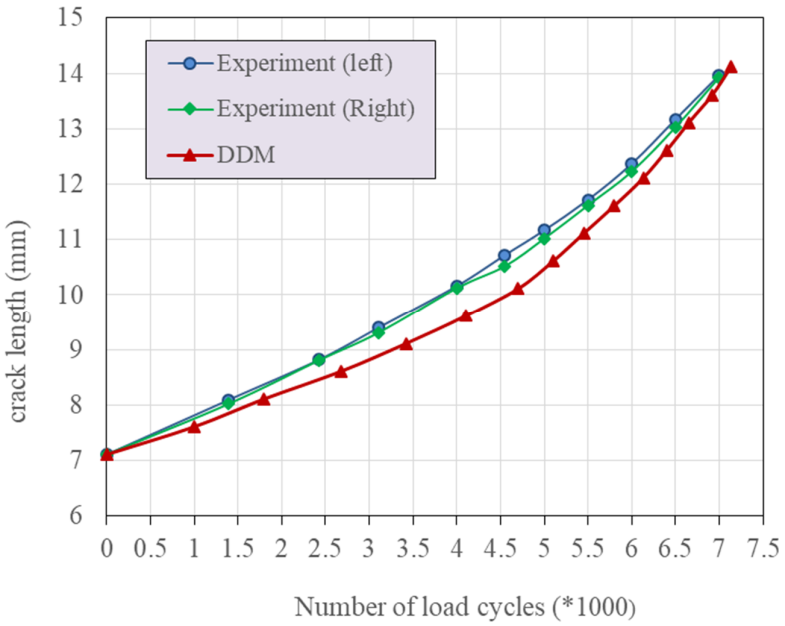

Figure 8. Life estimation of single crack under cyclic loading-incr of 0.5 mm.

4.2. Crack propagation in domain with two internal cracks

The second example considers the two internal, parallel crack propagation in the rectangular specimen. The dimension and boundary condition are represented in Figure 9a, and the length of the two cracks is $2a = 10\,mm$. The horizontal spacing between the two cracks is 15 mm, and the vertical spacing is 5 mm. A cyclic tensile load with a magnitude of 100 MPa is exerted at the upper

edge, while the displacements at the lower edge are restricted in both directions. This example contained four crack tips. Therefore, four crack tip elements were used along the crack surfaces (Figure 9b). Increments with a length of 2 mm were applied to perform the crack growth analysis. The material constants for the fatigue crack growth analysis are $C = 2.0 \times 10^{-8}$ and $m = 3.32$. The elasticity modulus, Poisson's ratios, fracture toughness, and threshold stress are considered as 74 GPa, 0.3, $60\,MPa\sqrt{m}$, and $2\,MPa\sqrt{m}$, respectively.

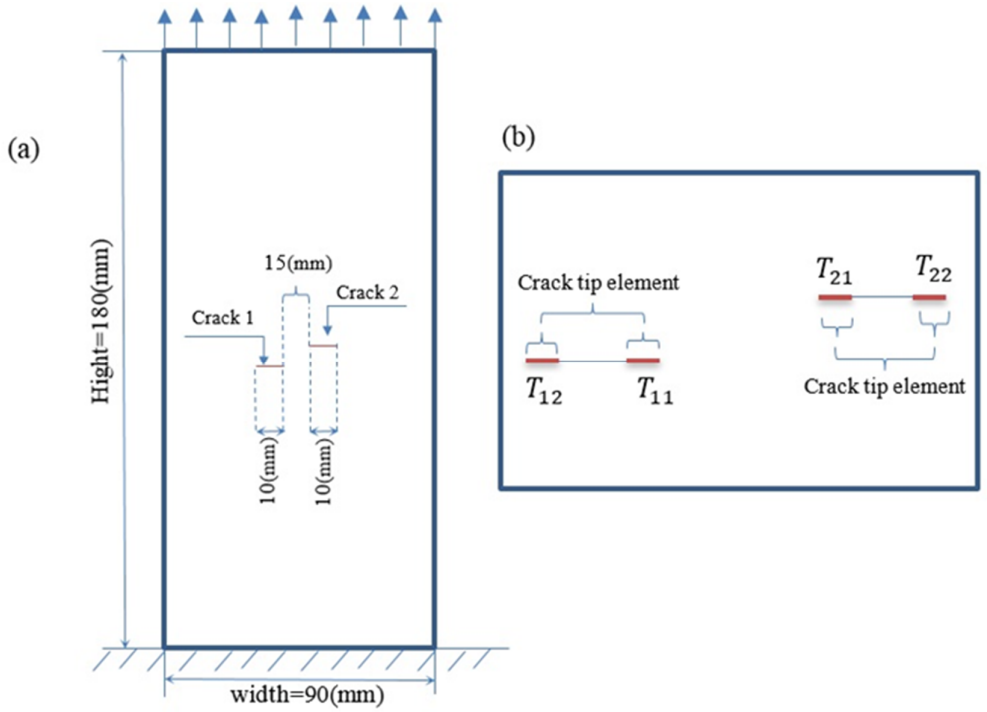

Figure 9. a) Tensioned specimen with two internal cracks, b) Magnification in cracks and crack tip element.

Figure 10. illustrates the crack path along 7 incremental growth. Each crack surface consists of two crack tip elements. Due to the symmetric conditions of the problem, the tips of the cracks are similar in pairs (T11-T21 and T12-T22). At the beginning of the growth process, all four crack tips show a similar initial growth rate. These conditions are observed in the first increment. After this step, the tips T11-T21 developed a higher growth rate than the tips T12-T22. Hence, different lengths of increment were allocated to both tips of a crack. As shown in Figure10, the length of crack development for each crack is less than 4 mm in one step. After the sixth growth step, the high values of the growth rate, and consequently, the higher growth increment belong to the crack tips T12-T22.

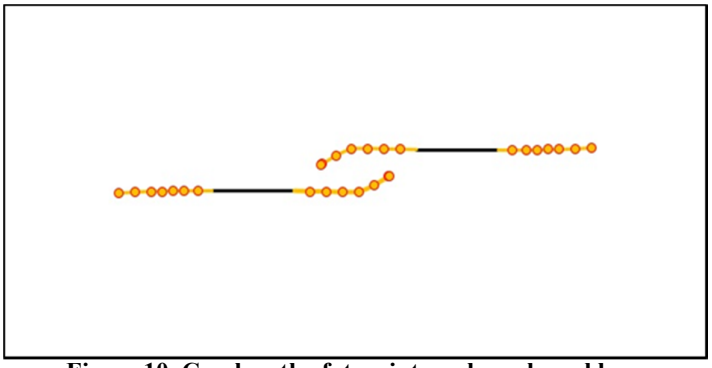

Figure 10. Crack path of two-internal crack problem.

The progress of the stress intensity factor values during the crack growth process is demonstrated in Figure 11, in which the curves indicated that mode-I was prevailing. At the initial propagation procedure, the ratio $|K_{II}|/K_I$, which is responsible for the crack growth deviations, is in the range of 0.003-0.02 for all crack tips. Besides, after the third increment, the crack tips T11 and T21 began to lean towards each other, and the ratio $|K_{II}|/K_I$ developed to 0.03-0.2. The increase in this ratio also caused the crack deviation. Figure 11 also presents the XFEM results [54]. The trend of all graphs is the same. The stress intensity factors values achieved by the proposed numerical approach are in good agreement with the values provided by XFEM for the tips T12-T22. Due to the deviation, the results of T11-T21 show slight differences.

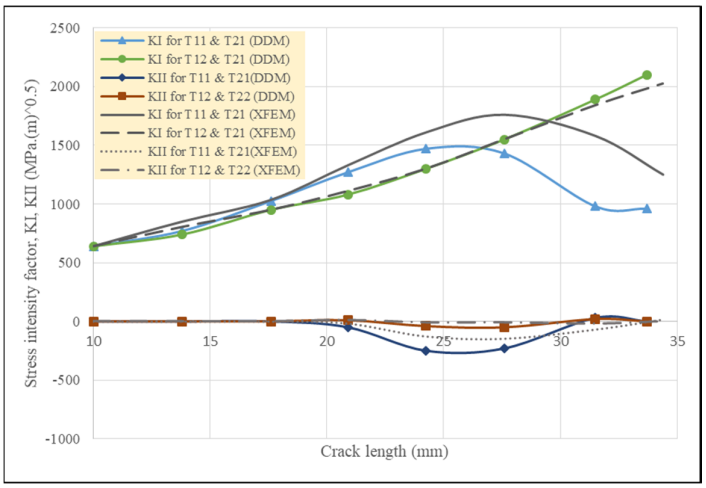

Figure 11. Stress intensity factor variation with crack length for two-internal crack problem.

Finally, Figure 12 illustrates the life acquired by the proposed numerical approach for two values of increment length (1 mm and 2 mm). In both results, the life of about 6500 load cycles was obtained. Good compliance was observed between the results of different increment lengths. Besides, Figure 12 includes the fatigue life curves for both crack tips (T11-T21, T12-T22) using XFEM, and life has been calculated separately for each crack tip. They show more cycles than DDM since the life prediction of the proposed method has been determined considering the crack tip with the highest growth rate at each growth step. This example exhibited the capability of the proposed numerical approach in simulating the fatigue crack growth of domains that included cracks that had different growth rates.

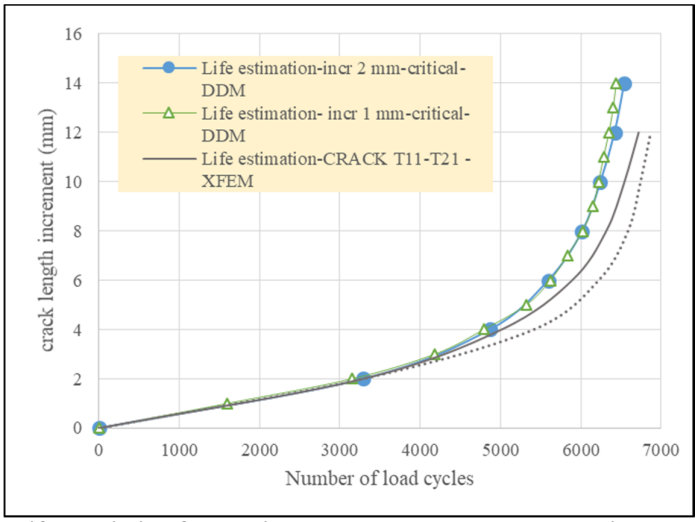

Figure 12. Specimen life prediction for two-internal crack problem-DDM, with two lengths of increment (1 mm and 2 mm), XFEM.

5. Conclusions

This work introduces a computational program through the displacement discontinuity method to accomplish the incremental crack propagation of cracked specimens under cyclic loading. The displacement discontinuity was utilized in order to evaluate the stress intensity factors. An experimental fatigue law was applied to model the crack incremental growth for domains that had cracked with different growth rates.

The crack path was determined using the maximum circumferential stress criterion. A correction procedure was used for this criterion in order to improve the crack propagation path. This system helps to obtain approximately a single growth path in the analysis with different incremental lengths. The correction angle depends on the increment of extension, and through this parameter, the growth angle of increment will be tangent to the continuous growth path of the crack. Indeed, utilizing this feature has made it possible to determine the growth path of crack fatigue more accurately.

Two examples were tested through the proposed method, demonstrating the performance in simulation of fatigue under cyclic load. The first was a case in which a single inclined crack was in the mixed-mode loading condition, and the other was considered as the two internal, parallel cracks that contained tips with different growth rates. This technique modeled the propagation of cracks with different growth rates in a domain accurately. Furthermore, the sensitivity of the results to the size of the increment was investigated. In the conditions that the modified σ -criterion was applied, the two lengths of initial increment indicated a good correlation in growth paths. Two different sizes caused low differences in life and crack growth direction. Indeed, this numerical technique has provided an accurate estimation of life (based on cycles) and mixed-mode fatigue cracks growth under cyclic loading by combining the DDM principles, fatigue laws, and appropriate growth path theory. Despite all the advantages of DDM, the limitation of this method must be considered in modeling the cracks with a lower growth rate. Besides, since the LEFM theory is applied for the crack growth process, the restrictions of this principle still govern the method. These issues can be the basis for a future research work.

References

[1]. Le, J.L., Manning, J. and Labuz, J.F. (2014). Scaling of fatigue crack growth in rock. Int J Rock Mech Min Sci. 72:71–9. https://doi.org/https://doi.org/10.1016/j.ijrmms.2014.08.015.

[2]. Li, G., Moelle, K.H.R. and Lewis, J.A. (1992). Fatigue crack growth in brittle sandstones. Int J Rock Mech Min Sci 29:469–77. https://doi.org/10.1016/0148-9062(92)92631-L.

[3]. Attewell, P.B. and Farmer, I.W. (1973). Fatigue behaviour of rock. Int J Rock Mech Min Sci Geomech Abstr. 10:1–9. https://doi.org/https://doi.org/10.1016/0148-9062(73)90055-7.

[4]. Richard, H.A. and Sander, M. (2016). Fatigue crack growth. Springer.

[5]. Liu, Y. and Dai, F. (2021). A review of experimental and theoretical research on the deformation and failure behavior of rocks subjected to cyclic loading. J Rock Mech Geotech Eng. 13:1203–30. https://doi.org/https://doi.org/10.1016/j.jrmge.2021.03.012.

[6]. Fan, J. (2017). Research on fatigue damage and dilatancy properties for salt rock under discontinuous cyclic loading. Chongqing University.

[7]. Dowling, N.E. (2009). Mechanical Behavior of Materials, Vol. 46, Pearson Education. https://doi.org/10.5860/choice.46-6830.

[8]. Al-Mukhtar, A.M. and Merkel, B. (2015). Simulation of the crack propagation in rocks using fracture mechanics approach. J Fail Anal Prev. 15:90–100. https://doi.org/10.1007/s11668-014-9907-2.

[9]. Chang, G., Hua, X., Zhang, J. and Li, P. (2021). The Mechanism of Rock Mass Crack Propagation of Principal Stress Rotation in the Process of Tunnel Excavation. Shock Vib. 4698368. https://doi.org/10.1155/2021/4698368.

[10]. Campbell, F.C. (2012). Fatigue and Fracture: Understanding the Basics. ASM International.

[11]. Shemirani, A.B., Haeri, H., Sarfarazi, V. and Hedayat, A. (2017). A review paper about experimental investigations on failure behaviour of non-persistent joint. Geomech Eng. 13:535–70. https://doi.org/10.12989/gae.2017.13.4.535.

[12]. Rao, B.N. and Rahman, S. (2000). An efficient meshless method for fracture analysis of cracks. Comput Mech. 26:398–408. https://doi.org/10.1007/s004660000189.

[13]. Pathak, H., Singh, A. and Singh, I.V. (2013). Fatigue crack growth simulations of 3-D problems using XFEM. Int J Mech Sci. 76:112–31. https://doi.org/10.1016/j.ijmecsci.2013.09.001.

[14]. Ammendolea, D., Greco, F., Lonetti, P., Blasi, P.N. and Pascuzzo, A. (2020). Crack growth propagation modeling based on moving mesh method and interaction

integral approach. Procedia Struct Integr. 28:1981–91. https://doi.org/10.1016/j.prostr.2020.11.022.

[15]. Boljanović, S. and Maksimović, S. (2011). Analysis of the crack growth propagation process under mixed-mode loading. Eng Fract Mech. 78:1565–76. https://doi.org/10.1016/j.engfracmech.2011.02.003.

[16]. Haeri, H., Sarfarazi, V., Yazdani, M., Shemirani, A.B. and Hedayat, A. (2018). Experimental and numerical investigation of the center-cracked horseshoe disk method for determining the mode I fracture toughness of rock-like material. Rock Mech Rock Eng. 51:173–85. https://doi.org/10.1007/s00603-017-1310-3.

[17]. Aliabadi, M.H. (2003). The boundary element method, volume 2, applications in solids and structures, Vol. 2, John Wiley and Sons. https://doi.org/10.1002/bate.200301300.

[18]. Cen, Z. and Maier, G. (1992). Bifurcations and instabilities in fracture of cohesive-softening structures: a boundary element analysis. Fatigue Fract Eng Mater Struct. 15:911–28. https://doi.org/10.1111/j.1460-2695.1992.tb00066.x.

[19]. Gerstle, W.H. (1986). Finite and boundary element modelling of crack propagation in two-and three dimensions using interactive computer graphics. Cornell University, ProQuest Diss Theses Ph.D.

[20]. Ingraffea, A.R., Blandford, G.E. and Liggett, J.A. (1983). Automatic modelling of mixed-mode fatigue and quasi-static crack propagation using the boundary element method. ASTM Spec, Tech, Publ, ASTM International. 407–26. https://doi.org/10.1520/stp37085s.

[21]. Doblare, M., Espiga, F., Gracia, L. and Alcantud, M. (1990). Study of crack propagation in orthotropic materials by using the boundary element method. Eng Fract Mech. 37:953–67. https://doi.org/10.1016/0013-7944(90)90020-H.

[22]. Wang, P.B. and Yao, Z. (2006). Fast multipole DBEM analysis of fatigue crack growth. Comput Mech. 38:223–33. https://doi.org/10.1016/j.mechrescom.2005.06.006.

[23]. Yan, X. (2006). A boundary element modeling of fatigue crack growth in a plane elastic plate. Mech Res Commun. 33:470–81. https://doi.org/10.1016/j.mechrescom.2005.06.006.

[24]. Portela, A., Aliabadi, M.H. and Rooke DP. (1993). Dual boundary element incremental analysis of crack propagation. Comput Struct. 46:237–47. https://doi.org/10.1016/0045-7949(93)90189-K.

[25]. Mi, Y. and Aliabadi, M.H. (1994). Three-dimensional crack growth simulation using BEM. Comput Struct. 52:871–8. https://doi.org/10.1016/0045-7949(94)90072-8.

[26]. Mi, Y. and Aliabadi, M.H. (1995). An automatic procedure for mixed-mode crack growth analysis. Commun Numer Methods Eng. 11:167–77. https://doi.org/10.1002/cnm.1640110210.

[27]. Citarella, R. and Cricrì, G. (2010). Comparison of DBEM and FEM crack path predictions in a notched shaft under torsion. Eng Fract Mech. 77:1730–49. https://doi.org/10.1016/j.engfracmech.2010.03.012.

[28]. Leonel, E.D. and Venturini, W.S. (2011). Multiple random crack propagation using a boundary element formulation. Eng Fract Mech. 78:1077–90. https://doi.org/10.1016/j.engfracmech.2010.11.012.

[29]. Li, J., Sladek, J., Sladek, V. and Wen, P.H. (2020). Hybrid meshless displacement discontinuity method (MDDM) in fracture mechanics: static and dynamic. Eur J Mech. 83:104023. https://doi.org/10.1016/j.euromechsol.2020.10402.

[30]. Crouch, S.L., Starfield, A.M. and Rizzo, F.J. (1983). Boundary Element Methods in Solid Mechanics. J Appl Mech. 50:704–5. https://doi.org/10.1115/1.3167130.

[31]. Fatehi Marji, M., Gholamnejad, J. and Eghbal, M. (2011). On the crack propagation mechanism of brittle substances under various loading conditions. 11th Int, Multidiscip, Sci, geo-conference. Albena, Bulg. 1:561-8. https://doi.org/10.5593/sgem2011/s02.131.

[32]. Haeri, H., Shahriar, K., Marji, M.F. and Moarefvand, P. (2013). Simulating the bluntness of TBM disc cutters in rocks using displacement discontinuity method. Proc, 13th Int, Conf, Fract, China. 2:1414-23.

[33]. Behnia, M., Goshtasbi, K., Fatehi Marji, M. and Golshani, A. (2012). The effect of layers elastic parameters on hydraulic fracturing propagation utilizing displacement discontinuity method. J Anal Numer Methods Min Eng. 2:1–13.

[34]. Haeri, H., Khaloo, A. and Marji, M.F. (2015). Experimental and numerical analysis of Brazilian discs with multiple parallel cracks. Arab J Geosci. 8:5897–908. https://doi.org/10.1007/s12517-014-1598-1.

[35]. Wen, P.H. (1996). Dynamic fracture mechanics: displacement discontinuity method. Southampton, United Kingdom Billerica, MA Comput Mech Publ Eng. 29.

[36]. Zhao, M., Dang, H., Fan, C. and Chen, Z. (2017). Extended displacement discontinuity method for an interface crack in a three-dimensional transversely isotropic piezothermoelastic bi-material. Part 1. Int J Solids Struct. 117:14–25. https://doi.org/10.1016/j.ijsolstr.2017.04.016.

[37]. Li, K., Jiang, X., Ding, H. and Hu, X. (2019). Three-Dimensional Propagation Simulation and Parameter Analysis of Rock Joint with Displacement Discontinuity Method. Math Probl Eng. https://doi.org/10.1155/2019/3164817.

[38]. Haeri, H., Khaloo, A.R., Shahriar, K., Fatehi Marji, M.

and Moarefvand, P.A. (2015). Boundary element analysis of crack-propagation mechanism of micro-cracks in rock-like specimens under a uniform normal tension. J Min Environ. 6:73–93. https://doi.org/10.22044/jme..2015.362.

[39]. Marji, M.F. Simulation of crack coalescence mechanism underneath single and double disc cutters by higher order displacement discontinuity method. (2015). J Cent South Univ. 22:1045–54. https://doi.org/10.1007/s11771-015-2615-6.

[40]. Fatehi Marji, M. and Hosseini-Nasab, H. (2005). Application of higher order displacement discontinuity method using special crack tip elements in rock fracture mechanics. 20th World Min, Congr, Expo, Tehran, Iran. 699–704.

[41]. Haeri, H. Experimental crack analyses of concrete-like CSCBD specimens using a higher order DDM. (2015). Comput Concr. 16:881–96. https://doi.org/10.12989/cac.2015.16.6.881.

[42]. Haeri, H. Simulating the crack propagation mechanism of pre-cracked concrete specimens under shear loading conditions. (2015). Strength Mater. 47:618–32. https://doi.org/10.1007/s11223-015-9698-z.

[43]. Sih, G.C. (1974). Strain-energy-density factor applied to mixed mode crack problems. Int J Fract. 10:305–21. https://doi.org/10.1007/BF00035493.

[44]. Erdogan, F. and Sih, G.C. (1963). On the crack extension in plates under plane loading and transverse shear. J. Basic Eng. 85(4): 519-525. https://doi.org/10.1115/1.3656897.

[45]. Hussain, M.A, Pu, S.L. and Underwood, J. (1974). Strain energy release rate for a crack under combined mode I and mode II. Fract, Anal, Proc, Natl, Symp, Fract, Mech, part II, ASTM International. 2:2-27. https://doi.org/10.1520/stp33130s.

[46]. Alneasan, M., Behnia, M. and Bagherpour, R. (2020). Applicability of the classical fracture mechanics criteria to predict the crack propagation path in rock under compression. Eur J Environ Civ Eng. 24:1761–84. https://doi.org/10.1080/19648189.2018.1485597.

[47]. Behnia, M., Goshtasbi, K., Fatehi Marji, M. and Golshani, A. (2012). On the crack propagation modeling of hydraulic fracturing by a hybridized displacement discontinuity/boundary collocation method. J Min Environ. 2. https://doi.org/10.22044/jme.2012.15.

[48]. Crouch, S.L. (1976). Solution of plane elasticity problems by the displacement discontinuity method. I. Infinite body solution. Int J Numer Methods Eng. 10:301–43. https://doi.org/10.1002/nme.1620100206.

[49]. Shou, K.J. and Crouch, S.L. (1995). A higher order displacement discontinuity method for analysis of crack problems. Int J Rock Mech Min Sci Geomech Abstr. 32: 49–55. https://doi.org/10.1016/0148-9062(94)00016-V.

[50]. Marji, M.F., Hosseini Nasab, H. and Kohsary, A.H. (2006). On the uses of special crack tip elements in numerical rock fracture mechanics. Int J Solids Struct. 43:1669–92. https://doi.org/10.1016/j.ijsolstr.2005.04.042.

[51]. Marji, M.F. and Dehghani, I. (2010). Kinked crack analysis by a hybridized boundary element/boundary collocation method. Int J Solids Struct. 47:922–33.

[52]. Paris, P. and Erdogan, F. (1963). A critical analysis of crack propagation laws. J Fluids Eng Trans ASME. 85:528–33. https://doi.org/10.1115/1.3656900.

[53]. Pustejovsky, M.A. (1979). Fatigue crack propagation in titanium under general in-plane loading I: experiments. Eng Fract Mech. 11:9–15. https://doi.org/10.1016/0013-7944(79)90025-0.

[54]. Alshoaibi AM and Fageehi YA. Simulation of Quasi-Static Crack Propagation by Adaptive Finite Element Method. Metals (Basel) 2021;11:98. https://doi.org/10.3390/met11010098.

روش المان مرزی غیر مستقیم اصلاح شده برای تعیین رفتار خستگی مواد شبه سنگی بر مبنای مکانیک شکست الاستیسیته خطی

رضوان علیزاده[۱]، محمد فاتحی مرجی[۱*]، ابوالفضل عبدالهی‌پور[۲] و مهدی پورقاسمی ساغند[۱]

۱- دانشکده مهندسی معدن و متالورژی، دانشگاه یزد، یزد، ایران
۲-دانشکده مهندسی معدن، دانشگاه تهران، تهران، ایران

ارسال ۲۰۲۱/۱۲/۰۱، پذیرش ۲۰۲۱/۱۲/۱۶

* نویسنده مسئول مکاتبات: mohammad.fatehi@gmail.com

چکیده:

در این مطالعه، یک روش موثر جهت مدل‌سازی انتشار ترک خستگی در محیط‌های شکننده الاستیک خطی، معرفی می‌شود. روش ناپیوستگی جابجایی در تحلیل مورد استفاده قرار می‌گیرد و به منظور پیش‌بینی ضرایب شدت تنش مجاور نوک ترک، مرزها با استفاده از المان‌های درجه دوم گسسته‌سازی می‌گردد. این روند با استفاده از اصول مکانیک شکست الاستیسیته خطی دو بعدی اجرا می‌شود. جهت محاسبه ضرایب شدت تنش مود ترکیبی، مقادیر ناپیوستگی جابجایی نرمال و برشی نوک ترک، مورد استفاده قرار می‌گیرد. رشد ترک تدریجی است و برای هر افزایش رشد، نیازی به فرایند مش‌بندی مجدد نیست. این روش به دلیل سادگی در مش‌بندی، نسبت به روش المان محدود برتری دارد. جهت رشد ترک با استفاده از تئوری حداکثر تنش اصلی محاسبه می‌گردد. در این تحلیل‌ها از یک روش تکرار، جهت تخمین مسیر صحیح انتشار ترک استفاده می‌شود. از این رو، طول‌های مختلف رشد تدریجی، تاثیری بر مسیر رشد ترک ندارد. نتایج چندین مثال با هندسه‌های متفاوت ارائه شده است تا کارایی روش را برای تجزیه و تحلیل رشد ترک خستگی نشان دهد. دقت نتایج نشان می‌دهد که این فرمولاسیون برای مدل‌سازی رشد ترک خستگی در شرایط بارگذاری مود ترکیبی مناسب است.

کلمات کلیدی: انتشار ترک خستگی، شرایط مود ترکیبی، محدوده ضریب شدت تنش، بارگذاری سیکلی.